Spin dynamics of a spin-orbit-coupled Bose-Einstein condensate in a shaken harmonic trap

Chaohua Wu, Jingtao Fan,* Gang Chen,† and Suotang Jia
State Key Laboratory of Quantum Optics and Quantum Optics Devices, Institute of Laser Spectroscopy, Shanxi University, Taiyuan 030006, China
and Collaborative Innovation Center of Extreme Optics, Shanxi University, Taiyuan, Shanxi 030006, China

(Received 13 August 2018; published 22 January 2019)

We propose a mechanism to realize nontrivial spin dynamics in a one-dimensional spin-orbit-coupled Bose-Einstein condensate by abruptly shaking the harmonic trap. Continuously varying the shaking strength, it is found that the Bose-Einstein condensate may exhibit exotic nonequilibrium spin dynamics. Specifically, at some special values of the shaking strength, the time-averaged spin polarization shows sharp resonant peaks, whereas it tends to be zero at any other positions. Furthermore, the spacings between any two nearest peaks depend only on the system parameters and are thus identical to each other. By simplifying this time-dependent system to an exactly solvable "quantum quench" model, we show that the essential physics behind the exotic spin dynamics comes from periodic suppressing and enhancing of the out-of-phase interference. It is further shown that the presented physical picture persists under weak atomic interactions. This work may shed light on the ongoing research of spin-based quantum control and quantum information.

DOI: 10.1103/PhysRevA.99.013617

I. INTRODUCTION

As the simplest but most important building block of quantum mechanics, quantum spin systems not only stand at the heart of modern fundamental physics but also underly lots of applications. Especially for the past few years, it has been an indispensable resource in quantum information processing such as quantum computing [1–4], quantum memory [5–8], and quantum sensing [9,10]. Therefore, a deep understanding of quantum spin dynamics has become the major pursuit of theorists and experimentalists. Instead of controlling spins directly by external Zeeman-type fields, spin-orbit coupling (SOC) mixes spins and orbits of a composite quantum system, opening a new avenue to manipulate spins via the motional degrees of freedom. Notable examples manifesting this mechanism include the electric-dipole spin-resonance technique [11–13] and magnetic-free spin filtering [14], which are usually built in spin-based semiconducting devices. Moreover, SOC is in charge of a lot of novel physical phenomena; for example, the spin Hall effect [15,16] and topological insulators [17,18], whose potential applications are clearly beyond spintronics.

On the other hand, the exciting breakthrough on the realization of a spin-orbit-coupled Bose-Einstein condensate (BEC) [19] offers another powerful platform to investigate the SOC-related physics with ultracold atoms [20–28]. Since relevant parameters are engineerable to a large degree, such a setting is able to exhibit much richer properties on its own right, apart from simulating physics which has already existed in solid-state systems. For example, it has been demonstrated that various new ground-state phases (e.g., stripe phase [29], supersolid [30–32], spin-polarized phase [33], etc.) emerge. Moreover, the negative-mass hydrodynamics [34,35] and novel dynamics of the spins [36–45] and the center of mass [25,46,47] can also be triggered.

In this paper, we predict an exotic nonequilibrium spin dynamics in a one-dimensional (1D) spin-orbit-coupled BEC, which is driven by a sudden shake of the harmonic trap [48–50]. It is found that the features of the spin dynamics depend crucially on the shaking strength. At some special values, the time-averaged spin polarization exhibits sharp resonant peaks, whereas it tends to be zero at any other positions. Furthermore, the spacings between any two nearest peaks depend only on the system parameters and are thus identical to each other. By simplifying this time-dependent system to an exactly solvable "quantum quench" model, we show that the essential physics behind the exotic spin dynamics comes from periodic suppressing and enhancing of the out-of-phase interference. Although the physical picture presented is based on a interaction-free assumption, it turns out to be robust against weak atomic interactions. This work may shed light on the ongoing research of spin-based quantum control and quantum information.

II. SYSTEM AND HAMILTONIAN

Similar to the benchmark experiment [19], the system in consideration is a spin-orbit-coupled BEC trapped in a harmonic potential. As shown in Fig. 1(a), while the atoms are assumed to be tightly confined in the y-z plane obeying $\omega_x \ll \{\omega_y, \omega_z\}$, where $\omega_i (i = x, y, z)$ is the trap frequency in the i direction, the atomic motion is only relevant along the x direction. Two hyperfine ground states, such as $|F = 1, m_F = -1\rangle$ and $|F = 1, m_F = 0\rangle$ for ^{87}Rb atoms, define respectively the spin-up and spin-down components of the BEC. These two ground states are further coupled by two

*bkxyfjt@163.com
†chengang971@163.com

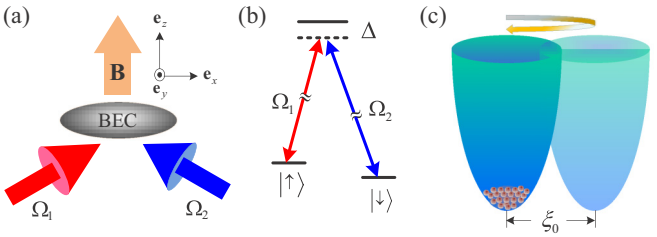

FIG. 1. (a) The proposed experimental setup. A 1D BEC (arranged in the x direction) is subject to two Raman lasers propagating in the x-y plane. A magnetic field $\mathbf{B}$ is applied along the z direction (b) The energy levels and their transitions. (c) A schematic description of the trap-shaking process. The definition of different labels is given in the main text.

counterpropagating Raman lasers, realizing a synthetic SOC, as shown in Fig. 1(b). Written in the dressed-state basis $|+\rangle = \exp(i\mathbf{k}_1 \cdot \mathbf{r})|\uparrow\rangle$ and $|-\rangle = \exp(i\mathbf{k}_2 \cdot \mathbf{r})|\downarrow\rangle$, with $\mathbf{k}_1$ and $\mathbf{k}_2$ being the wave vectors of the Raman lasers, the total dynamics can be described by the Gross-Pitaevskii equation

$$i\hbar\frac{\partial\Phi}{\partial t} = (H_S + H_I)\Phi, \tag{1}$$

where $\Phi = (\Phi_\uparrow, \Phi_\downarrow)^T$ is the spinor wave function. The single-particle Hamiltonian

$$H_S = \frac{p_x^2}{2m} + V(x,t) + \gamma p_x\sigma_z + \frac{\hbar\Omega}{2}\sigma_x, \tag{2}$$

where p_x and m are the atomic momentum and mass, respectively, $V(x,t) = m\omega_x^2[x - x_0(t)]^2/2$ is the trap potential, whose center $x_0(t)$ is intentionally assumed to be a time-dependent form, $\gamma = \hbar k/m$ defines the SOC strength with $k = |\mathbf{k}_1 - \mathbf{k}_2|/2 = \sqrt{2}\pi/\lambda$, $\Omega = \Omega_1\Omega_2/(2\Delta)$ describes the Raman coupling strength with Δ being the detuning from the excited state, and $\sigma_{x(z)}$ is the Pauli matrix. The nonlinear interaction between atoms is governed by the mean-field Hamiltonian

$$H_I = \begin{pmatrix} g_{\uparrow\uparrow}|\Phi_\uparrow|^2 + g_{\uparrow\downarrow}|\Phi_\downarrow|^2 & 0 \\ 0 & g_{\uparrow\downarrow}|\Phi_\uparrow|^2 + g_{\downarrow\downarrow}|\Phi_\downarrow|^2 \end{pmatrix}, \tag{3}$$

where $g_{\alpha\beta} = 4N\pi\hbar^2 a_{\alpha\beta}/(ml_y l_z)$ $(\alpha, \beta = \uparrow, \downarrow)$ is the effective 1D interaction parameter with $a_{\alpha\beta}$ being the s-wave scattering length between atoms in the hyperfine ground states, and $l_{y(z)} = \sqrt{\hbar/(m\omega_{y(z)})}$ [51,52]. Note that, in current experiments [33], $g_{\uparrow\downarrow} = g_{\downarrow\downarrow} \approx g_{\uparrow\uparrow} = g$.

The synthetic SOC hybridizes atomic spin and orbit degrees of freedom, enabling them behave in a collaborative fashion; it is therefore expected that the spin may sensitively respond to a time-dependent motional state. In the following discussion of this paper, we mainly engineer the time dependence of the trap potential to demonstrate an exotic spin dynamics.

We assume the BEC is somehow "kicked" at a certain time t_0. That is, one abruptly translates the harmonic trap along the x direction and then drags it back, as schematically shown in Fig. 1(c). Note that this process is completely determined by the expression of $x_0(t)$, which, without loss of generality, can be specified as a Gaussian profile, $x_0(t) = \xi_0 \exp[-(t - t_0)^2/\sigma_t^2]$, with ξ_0 and σ_t being the peak amplitude (shaking strength) and temporal width. The central idea is to monitor the spin dynamics activated by this sudden shake.

In the following numerical simulation, we rescale the Gross-Pitaevskii equation (1) with the energy, time, and length units $\hbar\omega$, ω^{-1}, and $\sqrt{\hbar/m\omega}$, respectively. We also replace ω_x by ω for simplicity.

III. SPIN DYNAMICS

In general, the coherent evolution of a quantum system is dominated by its single-particle Hamiltonian and the nonlinear interactions mostly contribute phase decoherence. To get a clearer physical picture underlying the coherent spin dynamics, we first address the case of $H_I = 0$.

Neglecting a dispensable constant and applying a unitary transformation by the operator $U = \exp[-im\omega^2 F(t)x/\hbar]$ with $F(t) = \int_0^t x_0(t)d\tau = F_0\{\mathrm{erf}[(t-t_0)/\sigma_t] + \mathrm{erf}(t_0/\sigma_t)\}/2$, where $F_0 = \sqrt{\pi}\sigma_t\xi_0$ and $\mathrm{erf}(x)$ is the error function, the Hamiltonian (2) turns into

$$H_S' = \frac{p_x^2}{2m} + \frac{1}{2}m\omega^2x^2 + \gamma p_x\sigma_z + \omega^2 F(t)p_x. \tag{4}$$

Note that, in writing the Hamiltonian (4), we have set $\Omega = 0$ to facilitate the following analyses and the influence of a finite Ω will be addressed later.

Due to the existence of $F(t)$, the Hamiltonian (4) still hampers an analytical solution, which necessitates a further approximation. To tackle this, we assume $\sigma_t \to 0$ and $\xi_0 \to \infty$, but let their product $F_0 = \sqrt{\pi}\sigma_t\xi_0$ remain invariant. In this limit, the time profile of $x_0(t)$ becomes a delta-type pulse and the corresponding time-dependent term tends to be $F(t) = F_0\Theta(t - t_0)$, where $\Theta(t - t_0)$ is the step function. That is, a time-dependent Hamiltonian problem is simplified to a model of quantum quench switched on at time t_0, which, fortunately, is exactly solvable. In the spirit of this, the dynamics in the time domains $t < t_0$ and $t > t_0$ are governed respectively by the time-independent Hamiltonians

$$\left.\begin{matrix} H_S'(t < t_0) \\ H_S'(t > t_0) \end{matrix}\right\} = \frac{p_x^2}{2m} + \frac{1}{2}m\omega^2x^2 + \gamma p_x\sigma_z + \begin{cases} 0 \\ \omega^2 F_0 p_x. \end{cases} \tag{5}$$

The eigenstates of the Hamiltonian (5) are given by

$$|\psi_{n,\sigma}\rangle = |\psi_n^\sigma\rangle|\sigma\rangle, \tag{6}$$

where $|\sigma\rangle$ is the eigenstate of the spin operator σ_z obeying $\sigma_z|\sigma\rangle = \sigma|\sigma\rangle$ with $\sigma = \pm$, and

$$|\psi_n^\sigma\rangle = \begin{cases} \exp\left(-\frac{i}{\hbar}m\gamma\sigma_z x\right)|\phi_n\rangle & (t < t_0) \\ \exp\left[-\frac{i}{\hbar}(m\gamma\sigma_z + m\omega^2F_0)x\right]|\phi_n\rangle & (t > t_0), \end{cases} \tag{7}$$

with $|\phi_n\rangle$ being the nth eigenstate of a harmonic oscillator. The corresponding eigenvalues are given by

$$E_{n,\sigma} = \begin{cases} n\hbar\omega - \frac{1}{2}m\gamma^2 & (t < t_0) \\ n\hbar\omega - \frac{1}{2}m\gamma^2 - \sigma m\omega^2\gamma F_0 - \frac{1}{2}m\omega^4F_0^2 & (t > t_0). \end{cases} \tag{8}$$

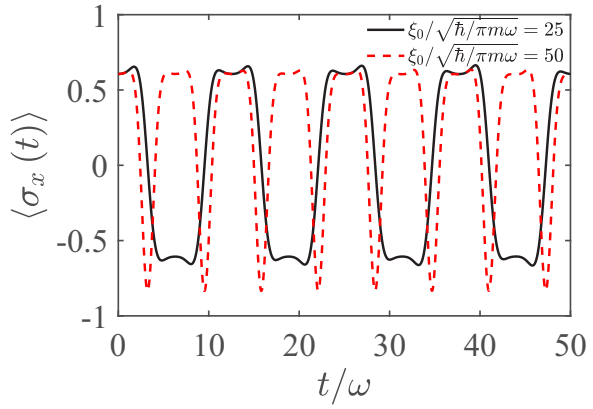

FIG. 2. Plot of $\langle\sigma_x(t)\rangle$ for $\xi_0/\sqrt{\hbar/\pi m\omega} = 25$ (black-solid curve) and $\xi_0/\sqrt{\hbar/\pi m\omega} = 50$ (red-dashed curve) with the initial state $|\Psi(0)\rangle = (|\psi_0^+\rangle|+\rangle + |\psi_0^-\rangle|-\rangle)/\sqrt{2}$. The other parameters are $\gamma = 0.2\sqrt{\hbar\omega/m}$ and $\sigma_t = 0.05/\omega$.

Equation (8) shows that, for $t < t_0$, the system is doubly degenerate with respect to spin reversion, say $E_{n,+} = E_{n,-}$. A sudden shake of the harmonic trap at t_0 lifts this degeneracy, leading to an energy splitting $E_{n,+} - E_{n,-} = -2m\omega^2\gamma F_0$. Thus, the evolution of a given state would accumulate a finite dynamical phase difference between different spin components, which opens up an interesting possibility to manipulate spin dynamics. To clarify this point, let us expand the time-dependent wave function in terms of the spin-orbit basis $|\psi_{n,\sigma}\rangle$ for $t > t_0$, i.e.,

$$|\Psi(t)\rangle = \sum_{n=0}^{\infty}\sum_{\sigma=\pm1} A_{n,\sigma}|\psi_{n,\sigma}\rangle \exp\left(-\frac{i}{\hbar}E_{n,\sigma}t\right), \qquad (9)$$

where $A_{n,\sigma} = \langle\psi_{n,\sigma}|\Psi(0)\rangle$ is the projected coefficient and $|\Psi(0)\rangle$ is any given initial state. With this wave function, we are now in a step to choose and investigate an appropriate physical observable which may exhibit nontrivial spin dynamics. Notice that due to SOC, any two spin-conserving orbit states are orthogonal, say $\langle\psi_n^\sigma|\psi_{n'}^\sigma\rangle = \delta_{n,n'}$, whereas the spin-reversed ones are not ($\langle\psi_n^\sigma|\psi_{n'}^{-\sigma}\rangle \neq 0$). This suggests that the spin polarization in the x direction, $\langle\sigma_x\rangle$, which mixes the spin states $|+\rangle$ and $|-\rangle$, is a promising candidate. A straightforward calculation shows that

$$\langle\sigma_x(t)\rangle = \sum_{n,n'=0}^{\infty}\sum_{\sigma,\sigma'=\pm1} R_{\sigma,\sigma'}(n,n') \times \exp\left[-\frac{i}{\hbar}(E_{n,\sigma} - E_{n',\sigma'})t\right], \qquad (10)$$

where $R_{+,-}(n,n') = A_{n,+}A_{n',-}^*\langle\psi_{n'}^-|\psi_n^+\rangle$, $R_{-,+}(n,n') = A_{n,-}A_{n',+}^*\langle\psi_{n'}^+|\psi_n^-\rangle$, $R_{-,-}(n,n') = A_{n,-}A_{n',-}^*\langle\psi_{n',-}|\sigma_x|\psi_{n,-}\rangle = 0$, and $R_{+,+}(n,n') = A_{n,+}A_{n',+}^*\langle\psi_{n',+}|\sigma_x|\psi_{n,+}\rangle = 0$.

As the dynamical phase factor in Eq. (10), $\exp[-i(E_{n,\sigma} - E_{n',\sigma'})t/\hbar]$, carries the control parameter F_0, we expect that a varying of the shaking strength may strongly impact the spin oscillations. Figure 2 plots $\langle\sigma_x(t)\rangle$ for various parameter with the initial state $|\Psi(0)\rangle = (|\psi_0^+\rangle|+\rangle + |\psi_0^-\rangle|-\rangle)/\sqrt{2}$. An important finding is that $\langle\sigma_x(t)\rangle$ has a symmetric oscillation around zero over time, for a general value of the shaking strength ξ_0. However, for some special values of ξ_0; for example, $\xi_0/\sqrt{\hbar/\pi m\omega} = 50$ as used in Fig. 2, the oscillation becomes asymmetric. This breaking of symmetry implies a more profound spin-resonant effect driven by the shake of trapping potential, motivating us to introduce the following time-domain-global quantity:

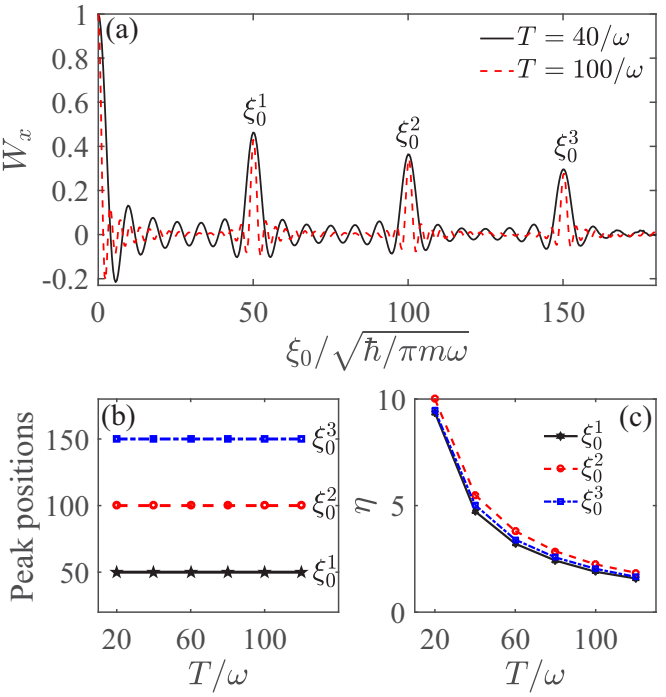

FIG. 3. (a) The long-time-averaged spin polarization W_x versus the shaking amplitude ξ_0 for $T = 40/\omega$ (black-solid curve) and $T = 100/\omega$ (blue-dotted curve). (b) The positions of resonant peaks varying with T. (c) The full widths at half maximum η of ξ_0^l ($l = 1, 2, 3$) versus T. The other parameters and the initial state are the same as those in Fig. 2.

$$W_x = \frac{1}{T}\int_{t_0}^{t_0+T}\langle\sigma_x(t)\rangle dt, \qquad (11)$$

where T is a long time span. In Fig. 3(a), we plot numerically W_x as a function of ξ_0 for the same initial state. Remarkably, despite of some minor oscillations, a series of sharp resonant peaks are periodically formed at

$$\frac{\xi_0}{\sqrt{\hbar/\pi m\omega}} = n \times 50 = 0, 50, 100, 150, \ldots. \qquad (12)$$

To understand the physics behind this effect, attention should be paid to the expression of Eq. (10). Observing $R_{\sigma,\sigma}(n,n') = 0$, the dynamical phases responsible for time oscillations are those of $-i(E_{n,\sigma} - E_{n',-\sigma})t/\hbar$, which are generally nonzero for a finite ξ_0. Therefore, $\langle\sigma_x(t)\rangle$ should average to zero after a long-time integration, due to the out-of-time interference. However, when ξ_0 is tuned to some specific values, such that $\xi_0^l = l\hbar\omega/(2\sqrt{\pi}\sigma_t m\omega^2\gamma)$ with $l = n - n'$, the corresponding oscillating frequencies, $E_{n,\sigma} - E_{n',-\sigma}$, vanish, giving rise to a huge nonzero contribution to W_x, and the resonant peaks thus emerge. We further note that the peak spacing, $\Delta\xi_{l,l+1} = \xi_0^{l+1} - \xi_0^l = \hbar\omega/(2\sqrt{\pi}\sigma_t m\omega^2\gamma)$, is

completely controlled by the system parameters irrespective of l, reflecting a potential capability in the implementation of precision measurement. Note that the analytical results of the peak positions are in strong agreement with the direct numerical simulation.

It should be noticed that the widths of the resonant peaks can be modulated by varying T. In Fig. 3(a), we plot W_x versus ξ_0 for two representative long-time spans, $T = 40/\omega$ and $T = 100/\omega$. It can be seen that a shorter T broadens the resonant peaks without impacting their positions, facilitating the experimental observations. A clearer manifestation can be found in Figs. 3(b) and 3(c), where the positions and the full widths at half maximum of the first three resonant peaks are respectively shown as functions of T.

The above analyses are general, in the sense that the choice of the initial state $|\Psi(0)\rangle$ is arbitrary to a large extent, provided that it is a superposition of $|+\rangle$ and $|-\rangle$. This superposition-state requirement, which is easy to be satisfied in current experiment [19], guarantees nonzero $R_{\sigma,\sigma'}(n, n')$ and the dynamics of $\langle\sigma_x(t)\rangle$ can thus be nontrivial.

Up to now, the discussions are restricted to the case where the Raman coupling and interaction terms are neglected. Considering, however, that both these terms are inevitable in an actual ultracold atom experiment, it is necessary to clarify their influence on the spin dynamics. We first address the role of the Raman coupling Ω. For the case where Ω is much less than the orbital splitting; namely, $\Omega \ll \omega$, we are allowed to use perturbation theory to get a quantitative understanding. After a straightforward calculation (see the appendix for details), the perturbed eigenenergies for $t > t_0$, which are accurate up to first order in Ω, can be summarized as

$$\tilde{E}_{n,\sigma} = \begin{cases} (n + k/2)\hbar\omega + \sigma q/2 \ (|E_{n,+} - E_{n+k,-}| \ll \hbar\omega) \\ E_{n,\sigma} \ \text{(otherwise)}, \end{cases} \tag{13}$$

where k is any integer number and $q = [(-k\hbar\omega + 2m\omega^2\gamma F_0)^2 + |\hbar\Omega\zeta|^2]^{1/2}$ with $\zeta = \langle\psi^+_{n+k}|\psi^-_n\rangle$. Note that we have neglected the dependence of q on n, since ζ is very small for any n and k. By requiring the oscillating frequencies $\tilde{E}_{n,\sigma} - \tilde{E}_{n,-\sigma}$ to be minimized, we derive the resonant shaking position $\xi_0^k = k\hbar\omega/(2\sqrt{\pi}\sigma_t m\omega^2\gamma)$, which is exactly the same as the one without Raman coupling. This quantitatively indicates that, at least as long as the perturbative picture holds, a weak Raman coupling does not affect the peak positions. To complement these analytical results, in Fig. 4(a) we numerically plot W_x versus ξ_0 for various Ω. Interestingly, whereas the width of each individual peak broadens for an increasing Ω, its position keeps invariant even for $\Omega/\omega = 0.5$, which is clearly out of the perturbative regime.

The impact of the atomic interactions is a bit different. In Fig. 4(b), we plot W_x versus ξ_0 for different g with $\Omega = 0$. This figure shows that, for weak g, the resonant peak structures, including their widths and positions, are almost unchanged. With further increasing g, the peaks are gradually smeared out from large ξ_0 to small ξ_0, due to the loss of phase coherence among different spin-orbit states, implying that the simple physical picture given above breaks down.

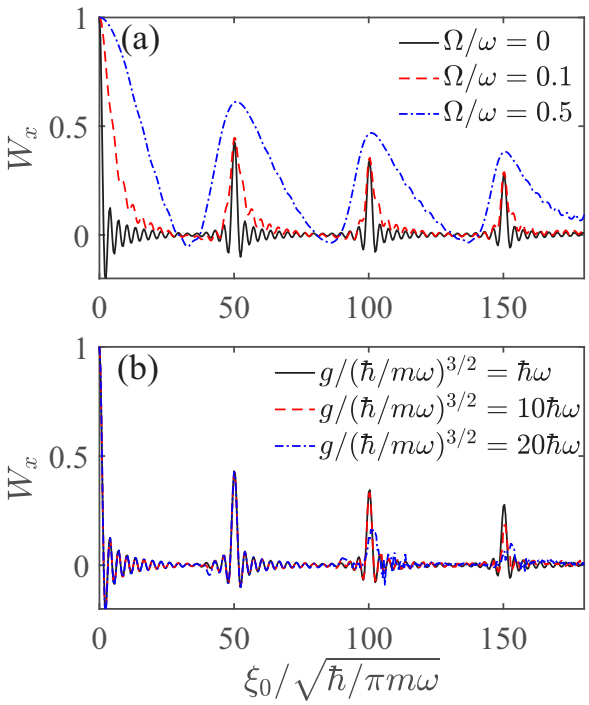

FIG. 4. The long-time-averaged spin polarization W_x versus the shaking amplitude ξ_0 for (a) $\Omega \neq 0$ and $g = 0$, (b) $\Omega = 0$ and $g \neq 0$. The time span is $T = 100/\omega$. The other parameters and the initial state are the same as those in Fig. 2.

IV. POSSIBLE EXPERIMENTAL IMPLEMENTATION

A possible experimental generation of the "trap shake" can be realized by applying an additional gradient magnetic field to the original harmonic-trapped BEC [53]. In light of this idea, the total trap potential is expressed as $V(x) = m\omega^2x^2/2 + \mu_B m_F g_F x\partial B/\partial x$, where μ_B is the Bohr magneton, m_F is the magnetic quantum number, g_F is the Landé factor, and $\partial B/\partial x$ is the field gradient. Thus, a sudden shake of the harmonic trap amounts to changing the gradient magnetic field accordingly.

We now give a brief estimation on the possible experimental parameters to show the feasibility of our proposal. For the BEC of ^{87}Rb atoms, the trap frequency can be set as $\omega \sim 2\pi \times 40$ Hz [25,33], from which the temporal width of shake is $\sigma_t = 0.05/\omega \approx 0.2$ ms and the long time span is assumed as $T = 40/\omega = 0.1$ s. In terms of the above parameters, the spacing between any two nearest peaks is estimated as $\Delta\xi_{l,l+1} = \hbar\omega/2\sqrt{\pi}\sigma_t m\omega^2\gamma \approx 718$ nm. These parameters show that our predicted spin dynamics and resonant effect can be observed in current experiments.

V. DISCUSSION

Note that, in this paper, we have assumed the BEC is confined only in the x direction. However, this is not a strict requirement. In fact, observing that the atomic motion degrees of freedom are decoupled in the x, y, and z directions, the geometry of BEC can be prepared as being either 1D, two dimensional, or three dimensional without affecting the above predictions.

Another crucial point one should keep in mind is that a quantum state collapses right after each detection. Therefore, a point-by-point measurement of $\langle\sigma_x(t)\rangle$ is actually based on independent trajectories [54,55]. That is to say, any individual point on the evolution curve of $\langle\sigma_x(t)\rangle$ does not necessarily come from the same initial state. To check the consistency of our theory with this, we formulate a random initial state $|\Psi(0)\rangle = \sum_{n=0}^{3}\sum_{\sigma=\pm1} c_{n,\sigma}|\psi_n^\sigma\rangle|\sigma\rangle$ for each experimental trajectory, where $c_{n,\sigma}$ is a random number in a given trajectory. It turns out that this kind of change does not influence the basic structure of W_x, including its peak positions.

VI. CONCLUSIONS

In summary, we have proposed a mechanism to realize nontrivial spin dynamics in a 1D spin-orbit-coupled BEC by abruptly shaking the harmonic trap. It has been found that the BEC may exhibit exotic nonequilibrium spin dynamics with respect to the shaking strength. Specifically, at some special values, the time-averaged spin polarization shows sharp resonant peaks, whereas it tend to be zero at any other positions. By simplifying this time-dependent system to an exactly solvable "quantum quench" model, we have shown that the essential physics behind the exotic spin dynamics comes from periodic suppressing and enhancing of the out-of-phase interference. It has been further demonstrated that the physical picture presented persists under weak atomic interactions.

ACKNOWLEDGMENTS

We would like to thank Prof. Jing Zhang for valuable discussions. This work was supported partly by the National Key R&D Program of China under Grant No. 2017YFA0304203; the NSFC under Grants No. 11674200, No. 11434007, and No. 11804204; and the PCSIRT under Grants No. IRT13076, No. SFSSSP, and No. 1331KSC.

APPENDIX: PERTURBATION THEORY FOR WEAK RAMAN COUPLING

Here we derive the perturbed eigenenergies and eigenstates in detail for small Raman coupling using perturbation theory. Note that the energy splitting of each degeneracy orbit state is proportional to the shaken strength, there exist a special case where the nth and $(n+k)$th orbits are degenerate or quasidegenerate, i.e., $|E_{n+k,+} - E_{n,-}| \ll \hbar\omega$, we must use degenerate perturbation theory in this case. Thus, the complete solutions should be divided into a nondegenerate case and a degenerate or quasidegenerate case.

Specifically, in the nondegenerate case, the eigenstate to the first-order correction is given by

$$|\varphi_{n,\sigma}\rangle = |\psi_n^\sigma\rangle|\sigma\rangle + \frac{\hbar\Omega}{2}\sum_{l\neq n}^{\infty}\frac{\langle\psi_l^{-\sigma}|\psi_n^\sigma\rangle}{(n-l)\hbar\omega - 2\sigma m\omega^2\gamma F_0} \times |\psi_l^{-\sigma}\rangle|-\sigma\rangle, \tag{A1}$$

with the perturbed eigenenergies $\tilde{E}_{n,\sigma} = E_{n,\sigma}$.

For the degenerate or quasidegenerate case, we assume the zeroth-order eigenstates for nth orbit state can be expressed in the form

$$|\varphi_n^{(0)}\rangle = a|\psi_n^-\rangle|-\rangle + b|\psi_{n+k}^+\rangle|+\rangle. \tag{A2}$$

By substituting the assumed eigenstate in Eq. (A2) into the Schrödinger equation $H_S|\varphi_n^{(0)}\rangle = \tilde{E}_n|\varphi_n^{(0)}\rangle$ and making use of $H_S'|\psi_n^\sigma\rangle|\sigma\rangle = E_{n,\sigma}|\psi_n^\sigma\rangle|\sigma\rangle$, we obtain

$$\begin{aligned}(E_{n,-} - \tilde{E}_n)a + \delta\zeta^* b = 0,\\ (E_{n+k,+} - \tilde{E}_n)b + \delta\zeta a = 0,\end{aligned} \tag{A3}$$

with $\zeta = \langle\psi_{n+k}^+|\psi_n^-\rangle$ and $\delta = \hbar\Omega/2$. The condition for the solution to Eq. (A3) is

$$\begin{vmatrix} E_{n,-} - \tilde{E}_n & \delta\zeta^* \\ \delta\zeta & E_{n+k,+} - \tilde{E}_n \end{vmatrix} = 0, \tag{A4}$$

which leads to

$$\tilde{E}_{n,\pm} = (n + k/2)\hbar\omega \pm q/2, \tag{A5}$$

with $q = [(-k\hbar\omega + 2m\omega^2\gamma F_0)^2 + 4\delta^2|\zeta|^2]^{1/2}$. The corresponding zeroth-order eigenstates are given by

$$|\varphi_{n,\pm}^{(0)}\rangle = a_{n,\pm}|\psi_n^-\rangle|-\rangle + b_{n,\pm}|\psi_{n+k}^+\rangle|+\rangle, \tag{A6}$$

with

$$a_{n,\pm} = \mp\frac{2\delta|\zeta|^2}{\sqrt{4\delta^2|\zeta|^2 + (k\hbar\omega + m\omega^2\gamma F_0 \pm q)}}, \tag{A7}$$

$$b_{n,\pm} = \frac{k\hbar\omega + m\omega^2\gamma F_0 \pm q}{\sqrt{4\delta^2|\zeta|^2 + (k\hbar\omega + m\omega^2\gamma F_0 \pm q)}}. \tag{A8}$$

According to the zeroth-order eigenstates and using the degenerate perturbation theory, the eigenstates to the first-order correction are written as

$$|\varphi_{n,\pm}\rangle = |\varphi_{n,\pm}^{(0)}\rangle + \sum_{l\neq n,n+k}^{\infty} S_1^\pm(l,n)|\psi_l^-\rangle|-\rangle + \sum_{l\neq n,n+k}^{\infty} S_2^\pm(l,n)|\psi_{l+k}^+\rangle|+\rangle, \tag{A9}$$

where

$$\begin{aligned}S_1^\pm(l,n) = {}& \frac{a_{l,+}}{E_{n,\pm} - E_{l,+}}(a_{l,+}b_{n,\pm}\langle\psi_l^-|\psi_{n+k}^+\rangle + a_{n,\pm}b_{l,+}\langle\psi_{l+k}^+|\psi_n^-\rangle)\\ &+ \frac{a_{l,-}}{E_{n,\pm} - E_{l,-}}(a_{l,-}b_{n,\pm}\langle\psi_l^-|\psi_{n+k}^+\rangle + a_{n,\pm}b_{l,-}\langle\psi_{l+k}^+|\psi_n^-\rangle),\end{aligned} \tag{A10}$$

and

$$S_2^{\pm}(l,n) = \frac{b_{l,+}}{E_{n,\pm} - E_{l,+}}(a_{l,+}b_{n,\pm}\langle\psi_l^-|\psi_{n+k}^+\rangle + a_{n,\pm}b_{l,+}\langle\psi_{l+k}^+|\psi_n^-\rangle) + \frac{b_{l,-}}{E_{n,\pm} - E_{l,-}}(a_{l,-}b_{n,\pm}\langle\psi_l^-|\psi_{n+k}^+\rangle + a_{n,\pm}b_{l,-}\langle\psi_{l+k}^+|\psi_n^-\rangle). \quad \text{(A11)}$$

[1] D. Loss and D. P. DiVincenzo, Quantum computation with quantum dots, Phys. Rev. A **57**, 120 (1998).

[2] X. Hu and S. Das Sarma, Spin-based quantum computation in multielectron quantum dots, Phys. Rev. A **64**, 042312 (2001).

[3] J. H. Wesenberg, A. Ardavan, G. A. D. Briggs, J. J. L. Morton, R. J. Schoelkopf, D. I. Schuster, and K. Mølmer, Quantum Computing with an Electron Spin Ensemble, Phys. Rev. Lett. **103**, 070502 (2009).

[4] C. Kloeffel and D. Loss, Prospects for spin-based quantum computing in quantum dots, Annu. Rev. Condens. Matter Phys. **4**, 51 (2013).

[5] A. I. Lvovsky, B. C. Sanders, and W. Tittel, Optical quantum memory, Nat. Photonics **3**, 706 (2009).

[6] C. Boehme and D. R. McCamey, Nuclear-spin quantum memory poised to take the lead, Science **336**, 1239 (2012).

[7] B. Julsgaard, C. Grezes, P. Bertet, and K. Mølmer, Quantum Memory for Microwave Photons in an Inhomogeneously Broadened Spin Ensemble, Phys. Rev. Lett. **110**, 250503 (2013).

[8] S. Zaiser, T. Rendler, I. Jakobi, T. Wolf, S.-Y. Lee, S. Wagner, V. Bergholm, T. Schulte-Herbrüggen, P. Neumann, and J. Wrachtrup, Enhancing quantum sensing sensitivity by a quantum memory, Nat. Commun. **7**, 12279 (2016).

[9] C. L. Degen, F. Reinhard, and P. Cappellaro, Quantum sensing, Rev. Mod. Phys. **89**, 035002 (2017).

[10] F. Poggiali, P. Cappellaro, and N. Fabbri, Optimal Control for One-Qubit Quantum Sensing, Phys. Rev. X **8**, 021059 (2018).

[11] R. L. Bell, Electric Dipole Spin Transitions in InSb, Phys. Rev. Lett. **9**, 52 (1962).

[12] E. I. Rashba and Al. L. Efros, Orbital Mechanisms of Electron-Spin Manipulation by an Electric Field, Phys. Rev. Lett. **91**, 126405 (2003).

[13] V. N. Golovach, M. Borhani, and D. Loss, Electric-dipole-induced spin resonance in quantum dots, Phys. Rev. B **74**, 165319 (2006).

[14] S. Bednarek, P. Szumniak, and B. Szafran, Spin accumulation and spin read out without magnetic field, Phys. Rev. B **82**, 235319 (2010).

[15] D. Xiao, M.-C. Chang, and Q. Niu, Berry phase effects on electronic properties, Rev. Mod. Phys. **82**, 1959 (2010).

[16] M. C. Beeler, R. A. Williams, K. Jiménez-García, L. J. LeBlanc, A. R. Perry, and I. B. Spielman, The spin Hall effect in a quantum gas, Nature (London) **498**, 201 (2013).

[17] M. Z. Hasan and C. L. Kane, Topological insulators, Rev. Mod. Phys. **82**, 3045 (2010).

[18] X.-L. Qi and S.-C. Zhang, Topological insulators and superconductors, Rev. Mod. Phys. **83**, 1057 (2011).

[19] Y.-J. Lin, K. Jiménez-García, and I. B. Spielman, Spin-orbit-coupled Bose-Einstein condensates, Nature (London) **471**, 83 (2011).

[20] C. Wang, C. Gao, C.-M. Jian, and H. Zhai, Spin-Orbit Coupled Spinor Bose-Einstein Condensates, Phys. Rev. Lett. **105**, 160403 (2010).

[21] Z. Fu, P. Wang, S. Chai, L. Huang, and J. Zhang, Bose-Einstein condensate in a light-induced vector gauge potential using 1064-nm optical-dipole-trap lasers, Phys. Rev. A **84**, 043609 (2011).

[22] C. Wu, I. Mondragon-Shem, and X.-F. Zhou, Unconventional Bose-Einstein condensations from spin-orbit coupling, Chin. Phys. Lett. **28**, 097102 (2011).

[23] S. Sinha, R. Nath, and L. Santos, Trapped Two-Dimensional Condensates with Synthetic Spin-Orbit Coupling, Phys. Rev. Lett. **107**, 270401 (2011).

[24] H. Hu, B. Ramachandhran, H. Pu, and X.-J. Liu, Spin-Orbit Coupled Weakly Interacting Bose-Einstein Condensates in Harmonic Traps, Phys. Rev. Lett. **108**, 010402 (2012).

[25] J.-Y. Zhang, S.-C. Ji, Z. Chen, L. Zhang, Z.-D. Du, B. Yan, G.-S. Pan, B. Zhao, Y.-J. Deng, H. Zhai, S. Chen, and J.-W. Pan, Collective Dipole Oscillations of a Spin-Orbit Coupled Bose-Einstein Condensate, Phys. Rev. Lett. **109**, 115301 (2012).

[26] C. Qu, C. Hamner, M. Gong, C. Zhang, and P. Engels, Observation of Zitterbewegung in a spin-orbit-coupled Bose-Einstein condensate, Phys. Rev. A **88**, 021604(R) (2013).

[27] A. J. Olson, S.-J. Wang, R. J. Niffenegger, C.-H. Li, C. H. Greene, and Y. P. Chen, Tunable Landau-Zener transitions in a spin-orbit-coupled Bose-Einstein condensate, Phys. Rev. A **90**, 013616 (2014).

[28] Z. Wu, L. Zhang, W. Sun, X.-T. Xu, B.-Z. Wang, S.-C. Ji, Y. Deng, S. Chen, X.-J. Liu, and J.-W. Pan, Realization of two-dimensional spin-orbit coupling for Bose-Einstein condensates, Science **354**, 83 (2016).

[29] H. Zhai, Degenerate quantum gases with spin-orbit coupling, Rep. Prog. Phys. **78**, 026001 (2015).

[30] J.-R. Li, J. Lee, W. Huang, S. Burchesky, B. Shteynas, F. Ç. Top, A. O. Jamison, and W. Ketterle, A stripe phase with supersolid properties in spin-orbit-coupled Bose-Einstein condensates, Nature (London) **543**, 91 (2017).

[31] R. Liao, Searching for Supersolidity in Ultracold Atomic Bose Condensates with Rashba Spin-Orbit Coupling, Phys. Rev. Lett. **120**, 140403 (2018).

[32] W. Han, X.-F. Zhang, D.-S. Wang, H.-F. Jiang, W. Zhang, and S.-G. Zhang, Chiral Supersolid in Spin-Orbit-Coupled Bose Gases with Soft-Core Long-Range Interactions, Phys. Rev. Lett. **121**, 030404 (2018).

[33] C. Hamner, C. Qu, Y. Zhang, J. Chang, M. Gong, C. Zhang, and P. Engels, Dicke-type phase transition in a spin-orbit coupled Bose-Einstein condensate, Nat. Commun. **5**, 4023 (2014).

[34] M. A. Khamehchi, K. Hossain, M. E. Mossman, Y. Zhang, T. Busch, M. M. Forbes, and P. Engels, Negative-Mass

Hydrodynamics in a Spin-Orbit-Coupled Bose-Einstein Condensate, Phys. Rev. Lett. **118**, 155301 (2017).

[35] D. Colas, F. P. Laussy, and M. J. Davis, Negative-Mass Effects in Spin-Orbit Coupled Bose-Einstein Condensates, Phys. Rev. Lett. **121**, 055302 (2018).

[36] D. W. Zhang, L. B. Fu, Z. D. Wang, and S. L. Zhu, Josephson dynamics of a spin-orbit-coupled Bose-Einstein condensate in a double-well potential, Phys. Rev. A **85**, 043609 (2012).

[37] J. Larson, B. M. Anderson, and A. Altland, Chaos-driven dynamics in spin-orbit-coupled atomic gases, Phys. Rev. A **87**, 013624 (2013).

[38] Z. F. Yu and J. K. Xue, Selective coherent spin transportation in a spin-orbit-coupled bosonic junction, Phys. Rev. A **90**, 033618 (2014).

[39] J. Struck, J. Simonet, and K. Sengstock, Spin-orbit coupling in periodically driven optical lattices, Phys. Rev. A **90**, 031601(R) (2014).

[40] M. A. Garcia-March, G. Mazzarella, L. Dell'Anna, B. Julia Diaz, L. Salasnich, and A. Polls, Josephson physics of spin-orbit-coupled elongated Bose-Einstein condensates, Phys. Rev. A **89**, 063607 (2014).

[41] W.-Y. Wang, J. Liu, and L.-B. Fu, Measure synchronization in a spin-orbit-coupled bosonic Josephson junction, Phys. Rev. A **92**, 053608 (2015).

[42] Y. Li, C. Qu, Y. Zhang, and C. Zhang, Dynamical spin-density waves in a spin-orbit-coupled Bose-Einstein condensate, Phys. Rev. A **92**, 013635 (2015).

[43] S. Mardonov, M. Modugno, and E. Y. Sherman, Dynamics of Spin-Orbit Coupled Bose-Einstein Condensates in a Random Potential, Phys. Rev. Lett. **115**, 180402 (2015).

[44] T. F. J. Poon and X.-J. Liu, Quantum spin dynamics in a spin-orbit-coupled Bose-Einstein condensate, Phys. Rev. A **93**, 063420 (2016).

[45] J. Hou, X.-W. Luo, K. Sun, T. Bersano, V. Gokhroo, S. Mossman, P. Engels, and C. Zhang, Momentum-Space Josephson Effects, Phys. Rev. Lett. **120**, 120401 (2018).

[46] Y. Zhang, L. Mao, and C. Zhang, Mean-Field Dynamics of Spin-Orbit Coupled Bose-Einstein Condensates, Phys. Rev. Lett. **108**, 035302 (2012).

[47] Y. Zhang, G. Chen, and C. Zhang, Tunable spin-orbit coupling and quantum phase transition in a trapped Bose-Einstein condensate, Sci. Rep. **3**, 1937 (2013).

[48] Y. Japha and Y. B. Band, Motion of a condensate in a shaken and vibrating harmonic trap, J. Phys. B: At., Mol. Opt. Phys. **35**, 2383 (2002).

[49] H. M. Price, T. Ozawa, and N. Goldman, Synthetic dimensions for cold atoms from shaking a harmonic trap, Phys. Rev. A **95**, 023607 (2017).

[50] X. Chen, R.-L. Jiang, J. Li, Y. Ban, and E. Y. Sherman, Inverse engineering for fast transport and spin control of spin-orbit-coupled Bose-Einstein condensates in moving harmonic traps, Phys. Rev. A **97**, 013631 (2018).

[51] T.-L. Ho, Spinor Bose Condensates in Optical Traps, Phys. Rev. Lett. **81**, 742 (1998).

[52] A. Widera, F. Gerbier, S. Fölling, T. Gericke, O. Mandel, and I. Bloch, Precision measurement of spin-dependent interaction strengths for spin-1 and spin-2 ^{87}Rb atoms, New J. Phys. **8**, 152 (2006).

[53] Y. Li, G. Feng, R. Xu, X. Wang, J. Wu, G. Chen, X. Dai, J. Ma, L. Xiao, and S. Jia, Magnetic levitation for effective loading of cold cesium atoms in a crossed dipole trap, Phys. Rev. A **91**, 053604 (2015).

[54] J. Estève, C. Gross, A. Weller, S. Giovanazzi, and M. K. Oberthaler, Squeezing and entanglement in a Bose–Einstein condensate, Nature (London) **455**, 1216 (2008).

[55] C. Gross, T. Zibold, E. Nicklas, J. Estève, and M. K. Oberthaler, Nonlinear atom interferometer surpasses classical precision limit, Nature (London) **464**, 1165 (2010).